Proceedings World Geothermal Congress 2000
Kyushu - Tohoku, Japan, May 28 - June 10, 2000

GAS EQUILIBRIA CONTROLLING H_2S IN DIFFERENT PHILIPPINE GEOTHERMAL FIELDS

Farrell Siega[1], Noel Salonga[1] and Franco D'Amore[2]
[1]PNOC-Energy Development Corporation, Fort Bonifacio, Makati City, Philippines
[2]Instituto Internazionale per le Ricerche Geotermiche, Piazza Solferino 2, 56126 Pisa, Italy

Key Words: gas equilibria, steam fraction, reservoir temperature, Philippine fields

ABSTRACT

The reservoir temperature and mass steam fraction "y" can be evaluated through the simultaneous use of two gas equilibria reactions. This approach has been applied in selected Philippine geothermal field with the objective of finding suitable gas equilibria reaction, which would best characterize each field. The previous work on gas equilibria deals with the use of Fischer-Tropsch-pyrite/magnetite (FT-HSH1) reactions. In this study, the correlation of Fischer-Tropsch with pyrite-hematite (FT-HSH2) and pyrite-pyrrhotite (FT-HSH3) reactions was considered which generated two additional grid diagrams. As in FT-HSH1, the variation in calculated reservoir parameters with time and the distribution of data points within the grid indicates reservoir processes such as steam addition and dilution by cooler fluids like reinjection fluid and meteoric water.

The evaluation indicates that FT-HSH2 gave good correlation in mature hydrothermal system such as Tongonan, Mahanagdong and Palinpinon. It generally reflects the reservoir condition in these fields. All three gas equilibria methods, however are not applicable in highly degassed system such as Mt. Apo. Likewise, it gave inconsistent trends in mature system where acid-SO_4 fluids are present such as in Mahanagdong-B, Bacon-Manito and Labo.

In magmatic systems such as Pinatubo, Biliran and Alto Peak, the developed gas equilibria methods were able to delineate the characteristics of fluids in these areas. Acidic wells with significant magmatic contribution indicated relatively high reservoir temperature but lower steam fraction. Those wells with neutral-pH fluids but high gas content generally showed high steam fraction but lower temperature.

1.0 INTRODUCTION

The previous works on gas equilibria deals with use of two gas reactions namely, the Fischer-Tropsch (breakdown of methane), and the pyrite-magnetite. D'Amore and Truesdell (1995) have demonstrated the significance of this method in providing effective reservoir processes monitoring, especially in vapor dominated fields or those which becomes vapor dominated after long period of exploitation.

Further study on gas equilibria deals with two more equilibrium reactions, which are the pyrite-hematite and the pyrite-pyrrhotite. With this, aside from the Fischer-Tropsch-pyrite-magnetite correlation (FT-HSH1), two additional correlations were developed namely, the Fischer-Tropsch-pyrite-hematite (FT-HSH2) and the Fischer-Tropsch-pyrite-pyrrhotite (FT-HSH3).

The developed gas equilibria methods were applied in different Philippine geothermal fields (Fig. 1) to determine which would best characterize each field. Among the fields considered in this study are those in: 1) magmatic hydrothermal systems like the Pinatubo, Biliran and Alto Peak; 2) mature hydrothermal systems such as the Tongonan, Palinpinon and Mahanagdong A; 3) highly degassed system such as Mt. Apo; and 4) fields with acid-SO_4 fluids such as the Bacon-Manito, Labo and Mahanagdong B.

2.0 THEORY

The study correlates chemical parameters, easily measured at surface discharges, with physical parameters at reservoir condition through the use of chemical reactions between gaseous species that are assumed to be in equilibrium. The development of such correlation takes into account the existence of two-phase condition and vaporization of the liquid phase. The limitations and assumptions discussed in earlier works on gas equilibria by D'Amore and Truesdell (1995) are also considered in this study.

The four equilibria reactions considered for this study are the Fischer-Tropsch (FT), pyrite-magnetite (HSH1), pyrite-hematite (HSH2) and pyrite-pyrrhotite (HSH3) described by the following stoichiometric reactions:

FT: $CH_4 + 2H_2O = CO_2 + 4H_2$ (1)
HSH1: $H_2 + 2H_2O + 3/2FeS_2 = 3H_2S + 1/2Fe_3O_4$ (2)
HSH2: $5/4H_2+3/2FeS_2+3/4Fe_2O_3+7/4H_2O = 3H_2S+Fe_3O_4$ (3)
HSH3: $FeS_2 + H_2 = FeS + H_2S$ (4)

For each chemical equilibrium considered, the thermodynamic equilibrium constant could be written in which the concentration of each species is represented by its partial pressure P_i in the vapor phase.

$\text{Log } K_{FT} = 4\log P_{H2} + \log P_{CO2} - \log P_{CH4} - 2\log P_{H2O}$ (5)
$\text{Log } K_{HSH1} = 3\log P_{H2S} - \log P_{H2} - 2\log P_{H2O}$ (6)
$\text{Log } K_{HSH2} = 3\log P_{H2S} - 5/4\log P_{H2} - 7/4\log P_{H2O}$ (7)
$\text{Log } K_{HSH3} = \log P_{H2S} - \log P_{H2}$ (8)

Using the mass action law equation, the above equilibrium relations of the reactions can be expressed in terms of the partial pressure of H_2O (D'Amore and Truesdell, 1995):

$$\text{Log } P_i = \log (n_i/n_{H2O}) - \log A_i + \log P_{H2O} \quad (9)$$

where (n_i/n_{H2O}) is the measured molar concentration of the gas "i" with respect to H_2O. The A_I for each gas species can be defined as a function of temperature and in-place steam

fraction "y". If y is defined as the fraction of steam present with the liquid in the reservoir, then:

$$A_i = y + (1 - y) / B_I \quad \text{at} \quad y \geq 0 \qquad (10)$$

If y is defined as the fraction of steam lost from the liquid in the reservoir, then:

$$A_i = 1 / (Bi (1 + y - yB_i)) \quad \text{at} \quad y < 0 \qquad (11)$$

B_i is the vapor-liquid distribution coefficient, the ratio of the concentration of each gas in the vapor and liquid phases. The values of the distribution coefficients, which are known functions of temperature (Giggenbach, 1980; D'Amore and Truesdel, 1988), are given by:

$$\text{Log } B_{CO2} = 4.7593 - 0.01092t \qquad (12)$$
$$\text{Log } B_{H2S} = 4.0547 - 0.00981t \qquad (13)$$
$$\text{Log } B_{CH4} = 6.0783 - 0.01383t \qquad (14)$$
$$\text{Log } B_{H2} = 6.2283 - 0.01403t \qquad (15)$$

for temperature range of 100-340^{o}C.

Inserting equation (9) for each Pi in the mass action law equations, and using suitable expression for the equilibrium constant K (Table 1), the following gas equilibria equations are developed:

$$FT = \log K_{FT} + 4\log A_{H2} + \log A_{CO2} - \log A_{CH4} - 2\log P_{H2O} \qquad (16)$$
$$HSH1 = \log K_{HSH1} + 3\log A_{H2S} - \log A_{H2} \qquad (17)$$
$$HSH2 = \log K_{HSH2} + 3\log A_{H2S} - 5/4\log A_{H2} \qquad (18)$$
$$HSH3 = \log K_{HSH3} + \log A_{H2S} - \log A_{H2} \qquad (19)$$

The graphical solution of equation (16), (17), (18) and (19) generates grid diagrams of FT-HSH1, FT-HSH2 and FT-HSH3. In the diagram, chemical parameters FT, HSH1, HSH2 and HSH3 are reported as coordinates while the physical parameters, temperature and steam fraction, produce a grid inside the diagram.

In each of the expression from (16) to (19), the left side can be further expressed as molar ratio of each gas species with respect to H_2O, as follows:

$$FT = 4\log H_2/H_2O + \log CO_2/H_2O - \log CH_4/H_2O \qquad (20)$$
$$HSH1 = 3\log H_2S/H_2O - \log H_2/H_2O \qquad (21)$$
$$HSH2 = 3\log H_2S/H_2O - 5/4\log H_2/H_2O \qquad (22)$$
$$HSH3 = \log H_2S/H_2O - \log H_2/H_2O \qquad (23)$$

The distribution of data points inside the grid diagram connotes certain reservoir processes. The previous works on FT-HSH by D'Amore and Truesdell (1995) established the following trends and interpretations:

- Increase T and decrease y
  - indicate contribution of fluid from a hotter and deeper source with high liquid saturation
- Increase T and increase y
  - apparent increase in temperature and y due to lateral source of steam, with a practically zero liquid saturation value and with a strong local accumulation of gas which did not react in a pure vapor phase
- Decrease T and decrease y
  - indicate local source of pure and low temperature water with no gas content as in the case of reinjection fluids or fast meteoric recharge.
- Decrease T and increase y
  - often tied to a decrease in H_2S/H_2O ratio which could be caused either by :
    a. recharge, from peripheral fluids rich in gas, which has undergone a relatively long residence time in the reservoir.
    b. sulfides precipitation caused by local over-production with blockage of the main fractures. In this case, the residual condensate is effectively rich in salts as to bring about precipitation of greater quantities of sulphides than the local production of H_2S. This phenomenon soon leads to an abrupt drop in flowrate, pressure and residual production volume of the reservoir.

3.0 APPLICATION

3.1 Magmatic Hydrothermal System

The geothermal fields of Pinatubo, Alto Peak and Biliran are examples of hydrothermal systems with large magmatic contributions. The main sources of permeability in these fields came from structures related to past volcanism, like craters, radial fractures or brecciation due to dyke intrusions.

Figure 2 shows the FT-HSH grid diagrams of selected wells located in each field. The developed gas equilibria methods were able to characterize the fluids in these areas. Moreover, it is evident that FT-HSH2, which is based on Fischer-Tropsch/pyrite-hematite reactions, seems to give the best correlation among the three gas equilibria methods in magmatic system.

In all three diagrams, production wells from Pinatubo and Biliran (PN1, PN2D, PN3D, BN3) with acid-Cl-SO_4 type of fluids clustered at the high temperature section of the grid with zero to negative *y* values. The geochemical model in each field showed that these wells are proximate to the identified center of the resource.

Along this area, high magmatic gas fraction was observed with production wells having high level of total discharge H_2S (>150 mmoles/100moles) and CO_2 (>1500 mmoles/100moles). The water discharge from these wells are characterize by a high content of SO_4 which could be the main source of acidity. The lower *y* values ($y \leq 0$) could reflect the deep upflowing single-phase liquid tapped by these wells.

In the case of Alto Peak wells directed towards the center of the resource with neutral-pH Cl waters, the following trends were observed: 1) AP1D which possibly tap only the upper steam zone cap indicated high *y* value but lower temperature, and 2) AP2D which tap the main upflowing fluids indicated higher temperature and *y* value close to zero.

3.2 Mature Hydrothermal System

Figures 3 and 4 show the FT-HSH grid diagrams of production wells in Tongonan and Palinpinon. These two fields are examples of mature hydrothermal systems with neutral-pH Cl type of fluids. The data points of the wells located in these two fields plotted inside the grid in all of the three gas equilibria methods. However, taking into account the present reservoir condition in these fields indicated by other geochemical parameters (i.e. Cl, $TSiO_2$, $\delta^{18}O$), the Fischer-Tropsch and pyrite-hematite equilibria seems to provide better correlation with temperature and reservoir steam fraction.

Take for example the case of Tongonan field in Figure 3. After several years of exploitation and with the increase in mass extraction in 1996-98 due to the commercial operation of other power plants, the Tongonan field is currently experiencing field wide pressure drawdown. The physical and chemical parameters suggest the expansion of highly two-phase zone across the field covering the Tongonan-1, Upper Mahiao and South Sambaloran sectors. At present, it is only in Malitbog sector where wells still discharge liquid-dominated fluid while the rest have fluid discharge that is either steam dominated or highly two-phase.

The distribution of data points in the FT-HSH2 diagram generally reflects this reservoir condition. Those wells affected by the pressure drawdown have indicated vapor gain of between 0.5-5.0 % while the Malitbog wells, Tongonan-1 wells near the RI sink, and South Sambaloran wells lying at the periphery of the field, still plotted close to y=0 line. The other two grid diagrams, FT-HSH1 and FT-HSH3 have not clearly indicated the above observations.

Likewise in Palinpinon field (Fig. 4), well OK5D located near the postulated upflow zone southwest of Puhagan in the vicinity of Lagunao Dome, and wells PN20D and PN32D, which tapped the expanded two-phase zone (produced by field pressure drawdown) indicated high temperature of 295^{o}C and steam fraction of 0.01. Well PN28D, affected by incursion of reinjection fluids, discharge degassed fluid (y=-0.001) with temperature of 230-240^{o}C.

In other mature systems where acid-SO_4 fluids are present such as in Mahanagdong, Bacon-Manito and Labo, acidic wells indicated inconsistent trends, which could be attributed to the following reasons: 1) equilibria of gases in wells with acidic discharge are not controlled by any of the gas equilibria reactions considered, and 2) the H_2 concentration in the discharge which could come not only from geothermal sources but from cathodic reaction of corrosion processes. The latter was not considered in the development of the three gas equilibria methods. However, similar to that in Tongonan and Palinpinon fields, FT-HSH2 likewise showed better correlation compared to FT-HSH1 and FT-HSH3.

Figure 5 shows the FT-HSH grid diagrams of Mahanagdong field. In both FT-HSH1 and FT-HSH3, most of the data points plotted outside of the grid. On the other hand, almost all of the data points are inside the FT-HSH2 grid. The wells located near the center of the resource (MG3D, MG5D and MG14D), which are all gassy wells, have shown vapor gain by as much as 5% while those in the outflow area have lost vapor of about 1%. The acid wells (MG9D, MG15D, MG20D, MG21D) plotted on the vapor gain side, which does not make sense since they are cooler and have liquid discharges.

For Bacman field (Fig. 6), all three gas equilibria methods indicate the following trends: 1) data points of wells located near the upwelling zone in Botong sector plotted at high temperature and positive y section of the grid, and 2) decreasing y and temperature values of wells drilled in the Palayang Bayan and Cawayan area depending on their proximity to the center of the resource. As in Mahanagdong wells, Bacman wells (PAL-2D, CN-2D) and Labo wells (LB1D, LB3D, LB5D) with acidic discharge likewise yield inconsistent y and temperature values.

3.2 Degassed Hydrothermal System

The Mt. Apo geothermal field is an example of a degassed hydrothermal system. The wells drilled in this area generally have total discharge CO_2<100 mmoles/100moles, H_2S<15 mmoles/100moles, CH_4 and H_2<1 mmoles/100moles except those wells which tap a vapour-cap atop the two-phase zone inside the Sandawa Collapse. Nevertheless, in the three diagrams in Figure 7, almost all of the data points from these wells plotted outside of the grid. This lead to the conclusion that in degassed system the three gas equilibria systems in this paper are not applicable.

4.0 CONCLUSIONS

The first work in gas equilibria involves only the Fischer-Tropsch and pyrite-magnetite reactions. Further study leads to the consideration of the reactions involving the pyrite-hematite and pyrite-pyrrhotite. The manipulation of these reactions generates grid diagrams where the chemical parameters are reported as coordinates while the physical parameters, temperatures and steam fractions, produce a grid inside the diagram.

The application of these methods in different Philippine geothermal fields indicates the following important points:

- FT-HSH1, FT-HSH2 and FT-HSH3 are not applicable in degassed system like Mt. Apo
- acidic wells in mature hydrothermal systems give inconsistent trends inside the grid diagram
- acidic wells in magmatic hydrothermal systems indicate high temperature and close to zero y values.

The comparison of the three gas equilibria methods showed that FT-HSH2 provides the better correlation in mature and magmatic systems. The trends indicated by FT-HSH2, are consistent with other geochemical parameters and could be an effective tool in reservoir processes monitoring.

REFERENCES

Bolaños, G.T. (1998). Mahanagdong geothermal field quarterly technical reports. PNOC-EDC Internal Report.

Candelaria, M.N.R. and Baltasar, A.S.J. (1993). Geochemical and isotopic investigation of Biliran geothermal discharges. PNOC-EDC Internal Report.

D'Amore F. and Truesdell A.H. (1988). A review of equilibrium constants for gaseous species of geothermal interest. Sci. Geol. Bull. v. 41, pp. 309-332.

D'Amore F. and Truesdell A.H. (1995). Correlation between liquid saturation and physical phenomena in vapor-dominated geothermal reservoirs. Proc. 1995 World Geothermal Congress, pp. 1927-1931.

Giggenbach, W.F. (1980). Geothermal gas equilibria. Geochim. Cosmochim. Acta v. 44, pp. 2021-2032.

Maturgo, O.M., (1996). Chemical characteristics of acid fluids in some PNOC geothermal fields. Proc. 17th Annual PNOC-EDC Geothermal Conference, pp. 111-117.

PNOC-EDC (1990). Mt. Pinatubo resource assessment. PNOC-EDC Internal Report.

PNOC-EDC (1994). Mindanao 1 Geothermal Project resource assessment update. PNOC-EDC Internal Report.

Salonga, N.D. (1996). The geochemistry of the thermal fluids in Alto Peak magmatic hydrothermal system Leyte, Philippines. PNOC-EDC Internal Report

Salonga, N.D., Auman, R.O., Alincastre, R.S., Siega, F.L., Pa-a, J.E., and Bolaños, G.T. (1996). Baseline chemistry of Tongonan Goethermal Field prior to Leyte-Cebu and Leyte-Luzon interconnections. PNOC-EDC Internal Report.

Seastres, J.S., Hermoso, D.Z., Candelaria, M.N.R., and Gerardo, J.Y. (1995). Application of geochemical techniques in evaluating the reservoir response to exploitation at palinpinon Geotehrmal Field, Philippines. Proc. 1995 World Geothermal Congress, pp. 1025-1030.

Siega, F.L., Salazar, A.T.N., and Dacillo, D.B. (1998). Tongonan geothermal field quarterly technical reports. PNOC-EDC Internal Report

Solis, R.P., Cabel, A.C., See, F.S., Candelaria, M.N.R., Buenviaje, M.M., and Garcia, S.E. (1994). Bacon-Manito Geothermal Production Field pre-exploitation baseline geochemistry data. PNOC-EDC Internal Report

Table 1. Equilibrium constant expressions as a function of temperature.

Equilibrium Reactions	a	b	c
K_{FT}	-4.330	-8048	4.635
K_{HSH1}	6.449	-6150	-0.412
K_{HSH2}	7.609	-6087	-0.412
K_{HSH3}	4.940	-2874	-
P_{H2O}	5.510	-2048	-

where: $\log K = a + b/(T^oK) + c\log(T^oK)$

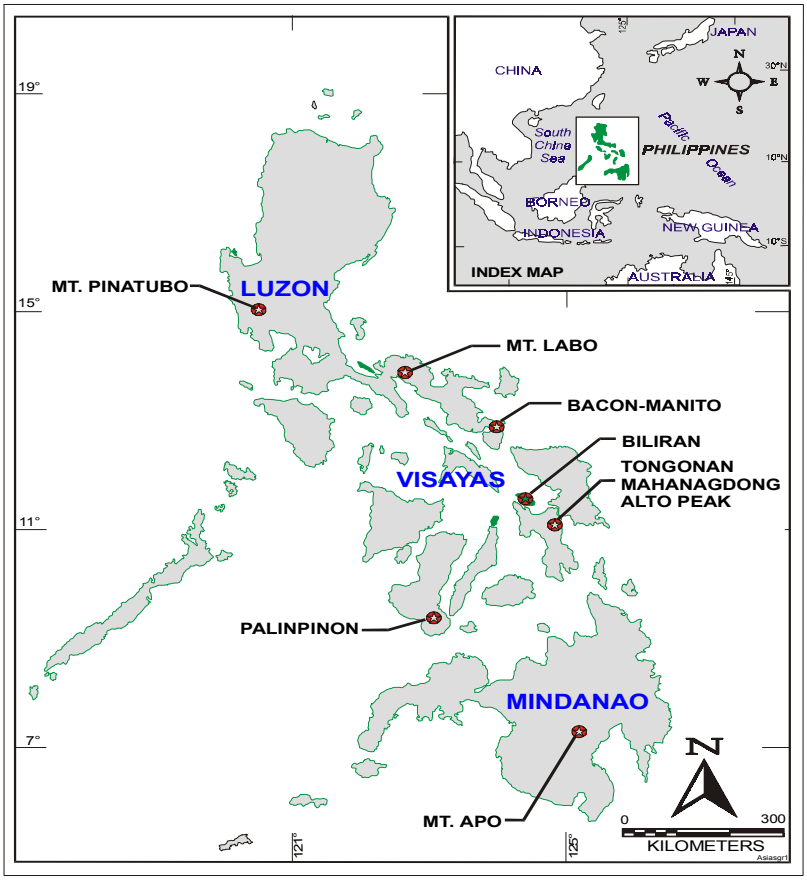

Figure 1. Map of the Philippines showing the location of geothermal fields included in the study

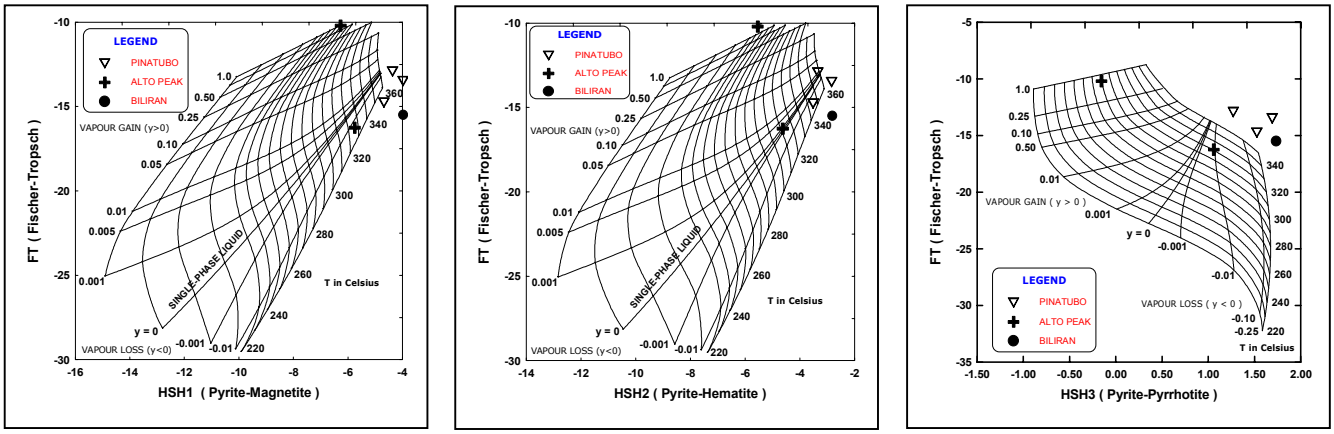

Figure 2. FT-HSH grid diagrams for Pinatubo, Biliran and Alto Peak wells.

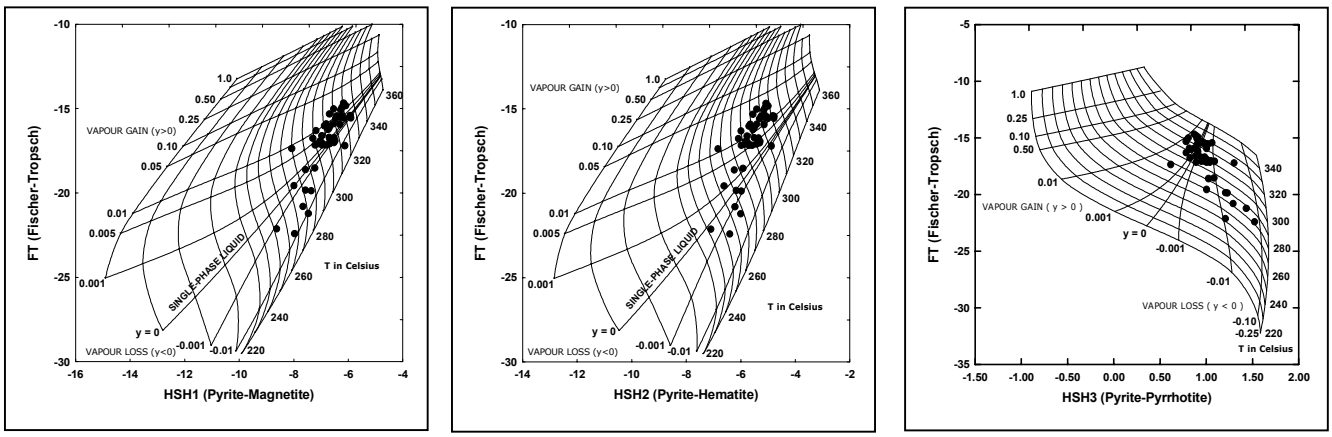

Figure 3. FT-HSH grid diagrams for Tongonan wells.

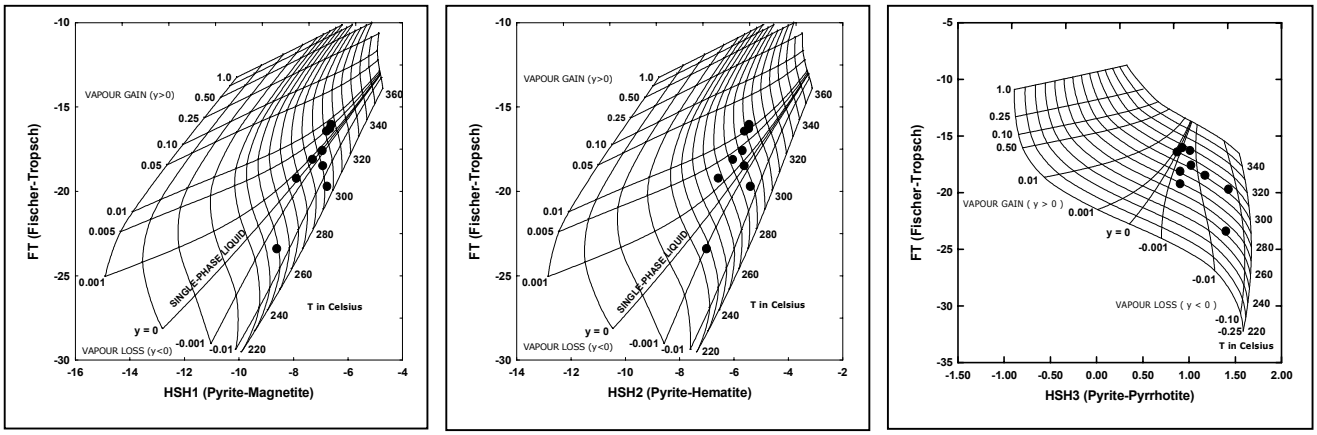

Figure 4. FT-HSH grid diagrams for Palinpinon wells.

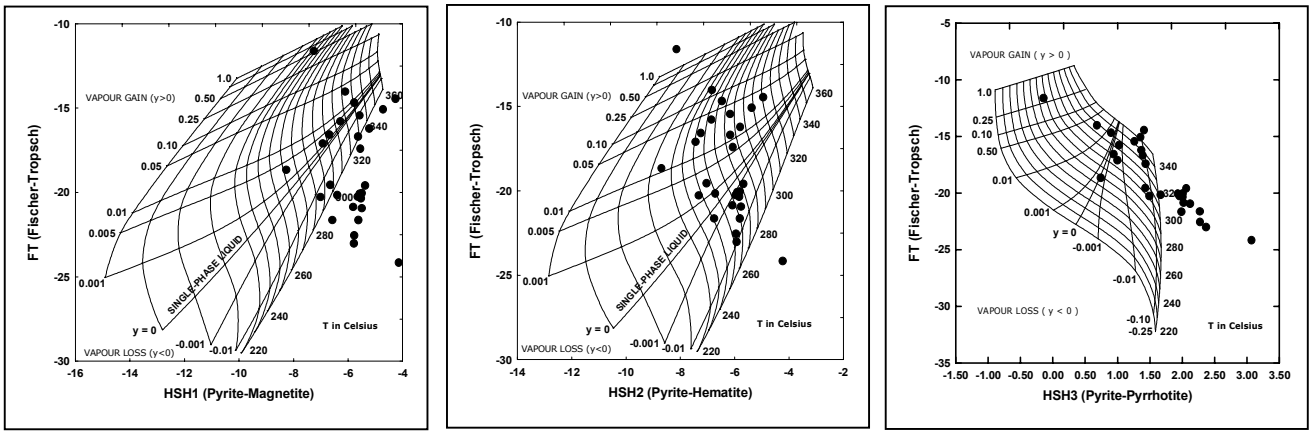

Figure 5. FT-HSH grid diagrams for Mahanagdong wells.

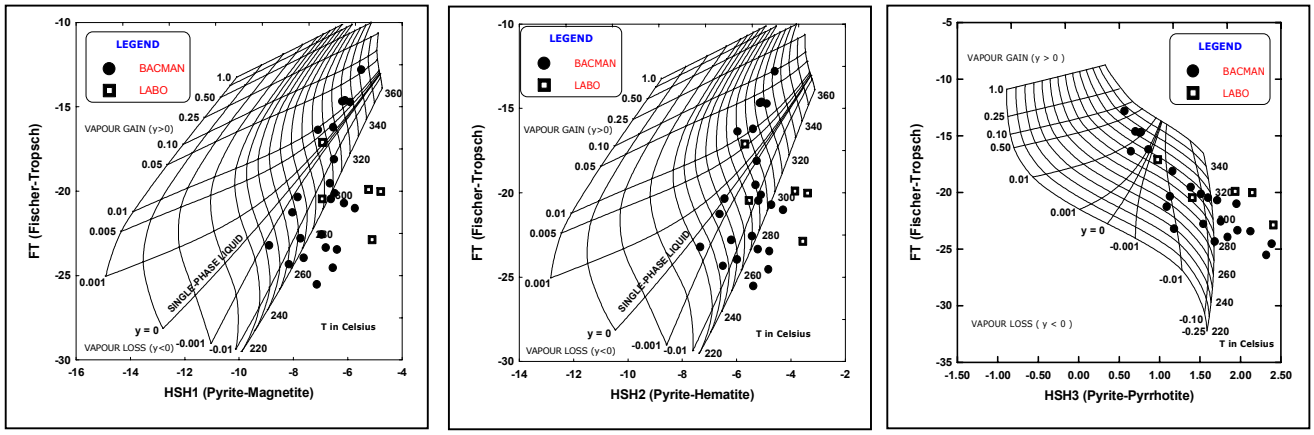

Figure 6. FT-HSH grid diagrams for Bacon-Manito and Mt. Labo wells.

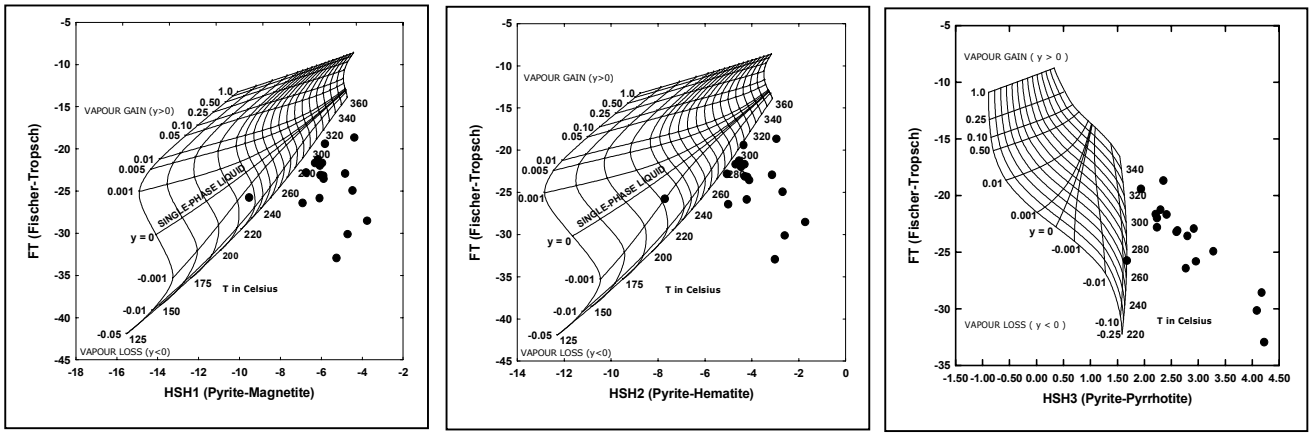

Figure 7. FT-HSH grid diagrams for Mt. Apo wells.